Escola de Primavera de Transição e Turbulência
Blumenau 2020

ABCM Associação Brasileira de Engenharia e Ciências Mecânicas

12th Spring School on Transition and Turbulence
September 21st-25th, 2020, Blumenau, SC, Brazil

EPTT-2020-0092
NUMERICAL SIMULATION OF THE PRIMARY BREAKUP IN A TWO-FLUID THIN NOZZLE

Lucas Ivan de Souza Vereza Medeiros
Rafael Vieira Velozo
Leonardo Machado da Rosa
Jonathan Utzig
Henry França Meier
Chemical Engineering Department – University of Blumenau
R. São Paulo, 3250, I-302 – 89030-000 Blumenau – Santa Catarina – Brazil
lucas.ivan.medeiros@gmail.com, rafael_velozo@hotmail.com, leorosa@gmail.com, jutzig@furb.br, meier@furb.br

Abstract. *The atomization phenomenon is recognized for its high complexity and the wide distribution of drop sizes, caused by the primary and secondary breakup that occurred in the formation of the droplets cloud, and has several industrial applications. Although this is a widely studied phenomenon, the atomization mechanisms are still not completely understood: the data acquisition in regions close to the dispersion nozzle is often limited. As a consequence, numerical studies associated with atomization are essential for a better understanding of the process. However, the small spatial and temporal scales of the phenomenon make numerical representation difficult due to the high computational effort required. Therefore, this study aims to propose a spatial simplification for simulating a two-fluid nozzle with a pseudo two-dimensional geometry, in order to make spray RANS simulations feasible. The working fluids considered for the spray simulations were air and water under supersonic conditions.With the use of the proposed approach, it is possible to employ more refined meshes and, consequently, obtain more detailed flow structures. Due to the nature of the proposed geometry, the comparison with experimental data obtained inside the nozzle becomes an alternative for the validation of the proposed modeling.*

Keywords: *sprays, two-fluid nozzle, primary breakup, computational fluid dynamics, pseudo two-dimensional geometry*

1. INTRODUCTION

Atomization is characterized by the disintegration of a jet or liquid sheet by its own kinetic energy, by the application of mechanical energy from vibrational or rotational equipment, or by contact with a high-speed gas stream (Lefebvre and Mcdonell, 2017). There are many processes in which the atomization phenomenon occurs (Verma *et al.*, 2017; Neto *et al.*, 2018; Ren *et al.*, 2019), aiming mainly to increase the liquid surface area, which provides greater heat and mass transfer and better mixing and evaporation conditions (Sinnamon *et al.*, 1980; Sanjosé *et al.*, 2011; Das and Lim, 2017; Bazdidi-Tehrani and Abedinejad, 2018).

The way in which the droplet dispersion is carried out directly influences the flow fluid dynamics and, in order to fully comprehend it, it is necessary to understand the development of the jet and the growth of small instabilities and disturbances (Lefebvre and Mcdonell, 2017). The primary breakup occurs in the region immediately after the liquid outlet of the nozzle, where the jets are destabilized by the aerodynamic interactions between the phases (Mäkelä, 2017). Oscillations in the interface are generated due to turbulent contact between liquid-gas phases, resulting in the formation of ligaments and the first droplets (Shinjo and Umemura, 2010). Thus, the nature of the primary breach is essentially dependent on operating conditions (Reitz, 1987). Although this is a widely studied phenomenon, the atomization mechanisms are still not completely understood: the data acquisition in regions close to the dispersion nozzle is often limited, which imposes difficulties in understanding the atomization mechanisms, particularly the primary breakup, a phenomenon inherently of random nature.

From a numerical point of view, atomization becomes a major challenge due to the coexistence of different scales of magnitude and, for a good representation, high mesh resolutions are required. Shinjo and Umemura (2010) numerically investigated the primary breakup of a liquid injected at high speed in stagnant air by a Direct Numerical Simulation (DNS) with a mesh resolution of 400 million to 6 billion elements. However, in cases where the gas phase is in more intense conditions, the computational effort required may make the simulation infeasible.

Xue and Kong (2009) developed a numerical mesh refinement methodology to maintain accuracy and minimize simulation time. The proposed refinement moves dynamically with the spray, causing the mesh size to increase in specific

places according to the imposed criterion. The study showed that the simulation with adaptive mesh obtained precision very similar to the case of the refined mesh globally, providing a computational effort saving.

Another alternative to reduce computational effort would be the conversion of small portions of liquid present in the Eulerian field into Lagrangian particles. These new particles – punctual and without volume – are injected in the position corresponding to the center of mass of the converted liquid structure. Sun *et al.* (2018) analyzed the breakup and evolution of the spray of a full-cone pressure swirl nozzle by a Reynolds Averaged Navier-Stokes (RANS) simulation, using the Euler-Lagrange approach on a mesh with 1.68 million elements. Simulations provided showed great consistency when comparing the resulting size and droplet velocity against the experimental measurements. Estivalèzes *et al.* (2018) developed a multi-scale approach for a RANS simulation of atomization of a planar liquid. The authors proposed an improved Euler-Lagrange coupling to guarantee a better transition between pure Eulerian and Lagrangian approaches and used adaptive mesh algorithms to dynamically optimize the mesh, obtaining a good qualitative comparison with experimental results.

According to Verma *et al.* (2017), simplifications in the geometry of the nozzle can lead to a reduction in the spatial domain and, consequently, in the simulation time. The authors carried out numerical and experimental studies to investigate the macroscopic structure of the spray and its characteristics generated by an internal-mix nozzle. The Volume of Fluid (VOF) model – where a single momentum equation is shared between the Eulerian phases in which its volumetric fractions are tracked across the domain – was used for interface recognition. The primary break-up was analysed within 2 mm from mixing point in a two-dimensional simulation to reduce computational effort. The initial diameter estimated by the two-dimensional simulation was used as an input to the Discrete Phase Model (DPM) in the three-dimensional domain after the region with continuous fluids mixing.

Regarding the studies carried out in our research group, Velozo (2020) determined a set of models and numerical methods capable of efficiently carrying out the RANS simulation of the primary breakup in a two-fluid nozzle used in the Fluid Catalytic Cracking process. For the same case study, Catapan (2020) evaluated secondary breakup models in RANS simulations with the Euler-Lagrange approach and analyzed the appropriate range of parameters for its study.

Therefore, this study aims to propose a spatial simplification for simulating a two-fluid nozzle with a pseudo two-dimensional geometry, in order to make RANS simulations of sprays feasible. With the use of this simplification, it is possible to employ more refined meshes and, consequently, obtain more detailed flow structures. The working fluids considered for the spray simulations were air and water under supersonic conditions. In the numerical simulations conducted, the VOF model was considered to describe the phases behavior, in which the geometric reconstruction method was used to track the interface. To describe the turbulent flow behavior, the SST k-ω model was used. The equations were solved using the finite volume method, available in a commercial simulator. This work is part of a larger project with an experimental study (Godoy *et al.*, 2020).

2. MATHEMATICAL MODELS

2.1 Euler-Euler approach

The Eulerian-Eulerian multiphase approach with surface-tracking by VOF model was used to describe the gas (g) and liquid phases (l). The continuity equation for each phase is calculated by Eqs. (1-2)

$$\frac{\partial}{\partial t}\left(\alpha_l \rho_l\right) + \nabla \cdot \left(\alpha_l \rho_l \mathbf{v}_l\right) = 0 \tag{1}$$

$$\frac{\partial}{\partial t}\left(\alpha_g \rho_g\right) + \nabla \cdot \left(\alpha_g \rho_g \mathbf{v}_g\right) = 0 \tag{2}$$

where α represents the volume fraction, ρ is the density, and $\mathbf{v}$ is the velocity vector.

In the VOF model, a single momentum equation (Eq. (3)) - which is dependent on the volume fractions of all phases through the properties ρ and μ - is solved, and the resulting velocity field is shared among the phases.

$$\frac{\partial}{\partial t}\left(\rho \mathbf{v}\right) + \nabla \cdot \left(\rho \mathbf{v}\mathbf{v}\right) = -\nabla p + \nabla \cdot \left[\mu_{ef}\left(\nabla \mathbf{v} + \nabla \mathbf{v}^T\right)\right] + \rho \mathbf{g} + \mathbf{F} \tag{3}$$

The surface tension force was determined from the Continuum Surface Stress (CSS) model (Eq. (4)).

$$F_{st} = \nabla \cdot \left(\sigma \left(|\alpha|\, I - \frac{\nabla \alpha \otimes \nabla \alpha}{|\nabla \alpha|}\right)\right) \tag{4}$$

where σ is the surface tension coefficient between two fluids and I is the unit tensor.

For cases with supersonic flows (where the effects of gas compressibility are considered), the energy conservation and density (ideal-gas) are resolved according to Eq. (5) and Eq. (6), respectively.

$$\frac{\partial}{\partial t}\left(\rho E\right) + \nabla \cdot \left(\mathbf{v}\left(\rho E + p\right)\right) = \nabla \cdot \left(k_{ef} \nabla T\right) + S_h \tag{5}$$

$$\rho = \frac{p\, exp\left(\frac{\int \frac{c_p}{T} dT}{R}\right) + p}{\frac{R}{MM} T} \tag{6}$$

where k_{ef} is the effective thermal conductivity shared by the phases, S_h is the source term, c_p is the heat capacity, R is the ideal gas constant, and MM is the molar mass.

In the VOF model, energy (E) and temperature (T) are treated as mass-averaged variables:

$$E = \frac{\alpha_l \rho_l E_l + \alpha_g \rho_g E_g}{\alpha_l \rho_l + \alpha_g \rho_g} \tag{7}$$

where E_l or E_l are based on the specific heat of that phase and the shared temperature.

2.2 Euler-Lagrange approach

An Eulerian-Lagrangian approach (DPM) between the gas phase and the droplets (p) was used with neglected particle-particle interactions. The force balance on the droplet is determined by Eq. (8).

$$\frac{d\mathbf{v}_p}{dt} = F_D\left(\mathbf{v}_g - \mathbf{v}_p\right) + \frac{\mathbf{g}\left(\rho_p - \rho_g\right)}{\rho_p} + \mathbf{F} \tag{8}$$

where $\mathbf{F}$ is an additional acceleration term and F_D is the drag force calculated by Eq. (9).

$$F_D = \frac{18\mu_g}{\rho_p {d_p}^2} \frac{C_D Re}{24} \tag{9}$$

with

$$Re = \frac{\rho d_p \left|v_p - v_g\right|}{\mu_g} \tag{10}$$

2.3 Turbulence modeling

According to Salvador *et al.* (2014) and Jubaer *et al.* (2019), the turbulence model proposed by Menter (1994) it is the most appropriate model to simulate problems involving atomization and sprays. In Menter's model, the conservation equations for turbulent kinetic energy (k) and the dissipation rate of turbulent kinetic energy (ω) are given by Eqs. (11-12).

$$\frac{\partial}{\partial t}(\rho k) + \nabla \cdot (\rho \mathbf{v} k) = \nabla \cdot \left[\left(\mu + \frac{\mu^t}{\sigma_k}\right) \nabla k\right] + \widetilde{P}_k - \beta^* \rho k \omega \tag{11}$$

$$\frac{\partial}{\partial t}(\rho \omega) + \nabla \cdot (\rho \mathbf{v} \omega) = \nabla \cdot \left[\left(\mu + \frac{\mu^t}{\sigma_\omega}\right) \nabla \omega\right] + \widetilde{C}_\alpha \frac{\omega}{k} P_k - \widetilde{C}_\beta \rho \omega^2 + 2\left(1 - F_1\right) \sigma_{\omega 2} \frac{\rho}{\omega} \nabla k \cdot \nabla \omega \tag{12}$$

where $\widetilde{C}_\alpha$, $\widetilde{C}_\beta$, and $\widetilde{P}_k$ are dependent on the blending functions as follows:

$$\widetilde{\phi} = F_1 \phi_1 + \left(1 - F_1\right) \phi_2 \tag{13}$$

The terms in Eqs. (11-12) are determined as follows:

- turbulent viscosity:

$$\mu^t = \frac{\rho a_1 k}{\max\left(a_1 \omega, \sqrt{2} S_t F_2\right)} \tag{14}$$

- strain rate magnitude:

$$S_t = \sqrt{\mathbf{S}_t \cdot \mathbf{S}_t} \tag{15}$$

$$\mathbf{S}_t = \frac{1}{2}\left(\nabla \mathbf{v} + \nabla \mathbf{v}^T\right) \tag{16}$$

- turbulent thermal conductivity:

$$k_t = \frac{\mu^t}{Pr_t} \tag{17}$$

- turbulent Prandtl numbers for k and ω:

$$\sigma_k = \frac{1}{\frac{F_1}{\sigma_{k,1}} + \frac{(1-F_1)}{\sigma_{k,2}}} \tag{18}$$

$$\sigma_\omega = \frac{1}{\frac{F_1}{\sigma_{\omega,1}} + \frac{(1-F_1)}{\sigma_{\omega,2}}} \tag{19}$$

- production of turbulence kinetic energy:

$$\widetilde{P}_k = \min\left(P_k, c_1\varepsilon\right) \tag{20}$$

$$P_k = \tau^{Re} : \nabla \mathbf{v} \tag{21}$$

- blending functions:

$$F_1 = \tanh\left({\gamma_1}^4\right) \tag{22}$$

$$\gamma_1 = \min\left(\max\left(\frac{\sqrt{k}}{\beta^*\omega\left(d_\perp\right)}, \frac{500\mu}{\left(d_\perp\right)^2\omega}\right), \frac{4\rho\sigma_{\omega 2}k}{CD_{k\omega}\left(d_\perp\right)^2}\right) \tag{23}$$

$$CD_{k\omega} = \max\left(2\rho\sigma_{\omega 2}\frac{1}{\omega}\nabla k \cdot \nabla\omega, 10^{-10}\right) \tag{24}$$

$$F_2 = \tanh\left({\gamma_2}^2\right) \tag{25}$$

$$\gamma_2 = \max\left(2\frac{\sqrt{k}}{\beta^*\omega\left(d_\perp\right)}, \frac{500\mu}{\left(d_\perp\right)^2\omega}\right) \tag{26}$$

where a_1, β^*, c_1, $C_{\alpha 1}$, $C_{\alpha 2}$, $C_{\beta 1}$, $C_{\beta 2}$, σ_{k1}, σ_{k2}, $\sigma_{\omega 1}$, $\sigma_{\omega 2}$, and Pr_t are constant, $d_\perp$ is the wall distance, and μ is the molecular viscosity.

3. NUMERICAL METHODOLOGY

In the numerical simulations conducted in the computational solver ANSYS® Fluent 19.1, the VOF method was considered to describe the phases behavior, in which the geometric reconstruction method (Youngs, 1982) was used to track the interface. The conversion of a portion of liquid from the Eulerian domain to Lagrangian points – considering the asphericity and maximum volume criteria – was determined based on the method proposed by Estivalèzes *et al.* (2018). To describe the turbulent flow behavior, the SST k-ω model was used (Menter, 1994). The governing equations was calculated using the finite volume method in conjunction with a second-order upwind scheme to discretize the advective terms and first-order schemes were kept to the other terms. For pressure-velocity coupling, the SIMPLEC algorithm was used. The adaptive mesh refinement method (Xue and Kong, 2009) was applied in a hexahedral mesh with 121,856 nodes (Fig. 1). The volume fraction gradient was considered for the refinement $\left(10^{-8}\right)$ and coarsening $\left(10^{-14}\right)$ criteria, with up to one level of refinement.

The boundary conditions used in the simulations are summarized as follows: the gas (atmospheric air in supersonic conditions) and liquid phase (water) are fed into their respective inlets (Fig. 1) with a prescribed mass flow rate (presented in Tab. 1); the discrete phase is injected into the domain only when the conversion criteria are accepted; a no-slip condition is applied at the nozzle walls; and the outlet surface has a zero pressure gradient boundary condition.

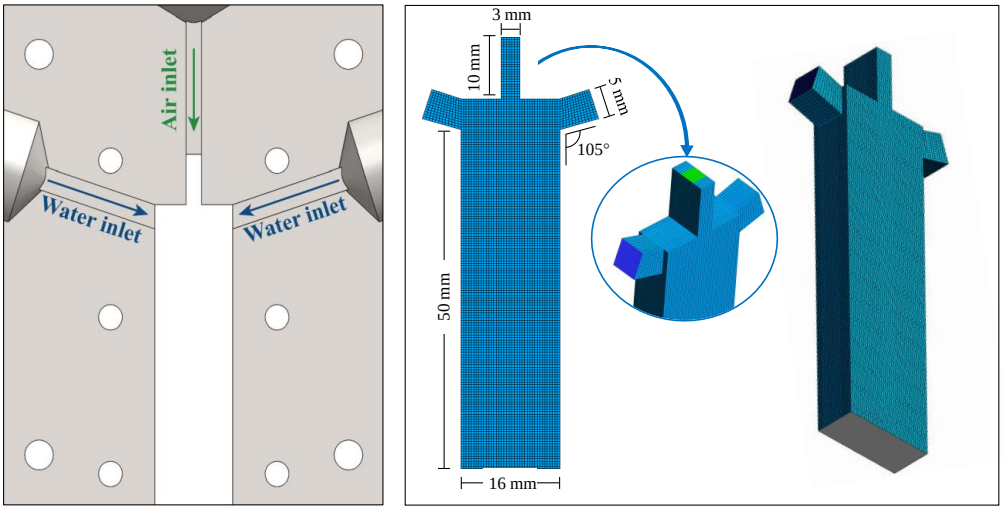

(a) (b)

Figure 1. (a) Geometry of the pseudo two-dimensional nozzle with a thickness of 10 mm. (b) Computational domain with a sampling plan (grey color) located at the outlet of the nozzle chamber.

Table 1. Operational conditions of the studied cases.

Case	Air flow rate (kg/h)	Water flow rate (kg/h)	Mass flow ratio
a[1]	40	365	9.12
b	50	1500	30.00
c	60	3000	50.00

[1]Operational condition used in Godoy *et al.* (2020).

4. RESULTS AND DISCUSSION

Figure 2 shows the volume fraction of the liquid phase and velocity contours for the studied cases after 0.100 s (Case a) or 0.036 s (Cases b and c), which are greater than the residence time of the respective case. It is possible to observe instabilities being formed in the interface regions, which occurs due to the contact between air at high velocity and water. The accumulation of the liquid in the regions close to the walls is considerably lower in Case a, which has the lowest flow ratio. For the cases with higher flow rates, this accumulation is increased. In Case a, in the regions above where the first contact between the phases occurs, the oscillations formed are smaller in size and quantity, as a result of the rapid rupture of the ligaments generated and, consequently, of the lower accumulation of liquid on the walls. It is also important to highlight that, despite the increase in gas flow rates during the experiments, the velocity magnitude decreases. This is due to the sharp pressure drop in the nozzle, which decreases proportionally to the mass ratio of the experiments, resulting in the velocity decrease.

Figure 3 shows that the liquid flowing through the edges of the nozzle chamber is not completely dismantled before leaving for the external environment. As a result, not only are droplets at the exit of the nozzle, but also large portions of liquid, which can still suffer the effects of the primary breakup. A visual comparison of the results of Cases a and c highlights that the increase in liquid flow directly influences the diameter distribution along the atomizer. It is possible to observe that smaller sizes and larger quantities of Lagrangian particles are obtained by simulation of the case of lower water flow rate. In order to compare the produced sizes distribution, Fig. 4 presents the distribution of Lagrangian droplet diameters at the nozzle outlet. It is observed that, even with greater gas flows, peaks of the distribution curves of Cases b and c are smaller and are slightly shifted to larger diameter intervals when compared to Case a. This result is directly related to the increase in liquid flow, reaffirming its influence on the droplet size. Another observed behavior in Fig. 3 is that the conditions with higher flow ratio resulted in the partial filling of the air inlet in the atomizer with water.

In order to investigate the turbulent behavior of the flow due to variations in mass flow ratio, the turbulent kinetic energy distributions are given in the Fig. 5. Such energy acts as the main driving force in the breaking of small portions of liquid into droplets, in other words, the interface regions where there is turbulent kinetic energy have the potential to occur the primary breakup. Analyzing Case a, the way in which the turbulent kinetic energy is distributed indicates that there are more regions with instabilities at the interface (when compared to the other cases). Consequently, it is expected that more Lagrangian particles will be generated with smaller sizes, which is proven in Figs. (2)-(3). The results also show

that the turbulent kinetic energy distribution is directly related to the amount of liquid present in the nozzle chamber: the intense concentration of liquid in Case c, for example, acts as an obstacle to air even at high speed, which makes it difficult to convert the kinetic energy associated with the flow into instability at the interface.

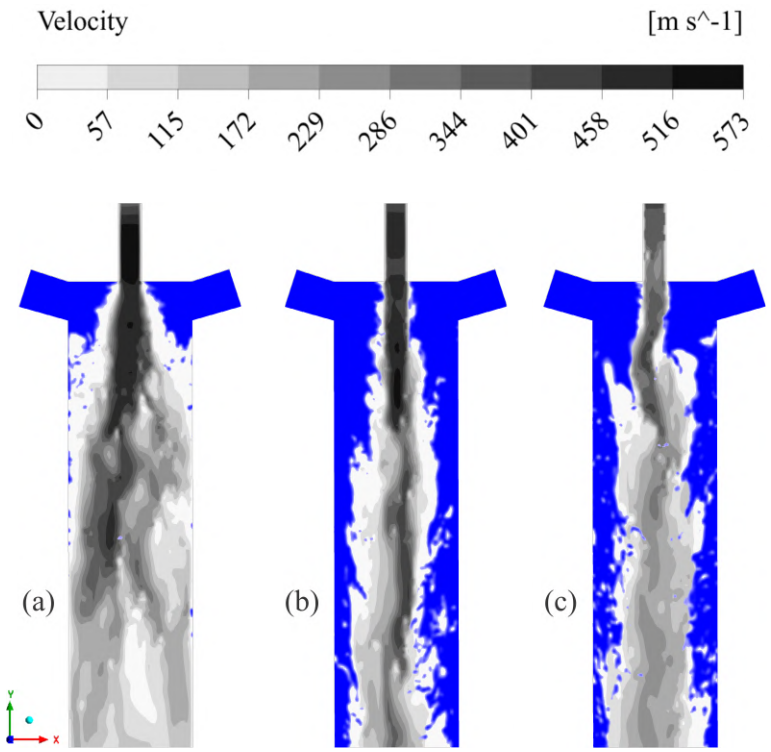

Figure 2. Volume fraction of liquid (blue color) and velocity contours for Cases a, b and c.

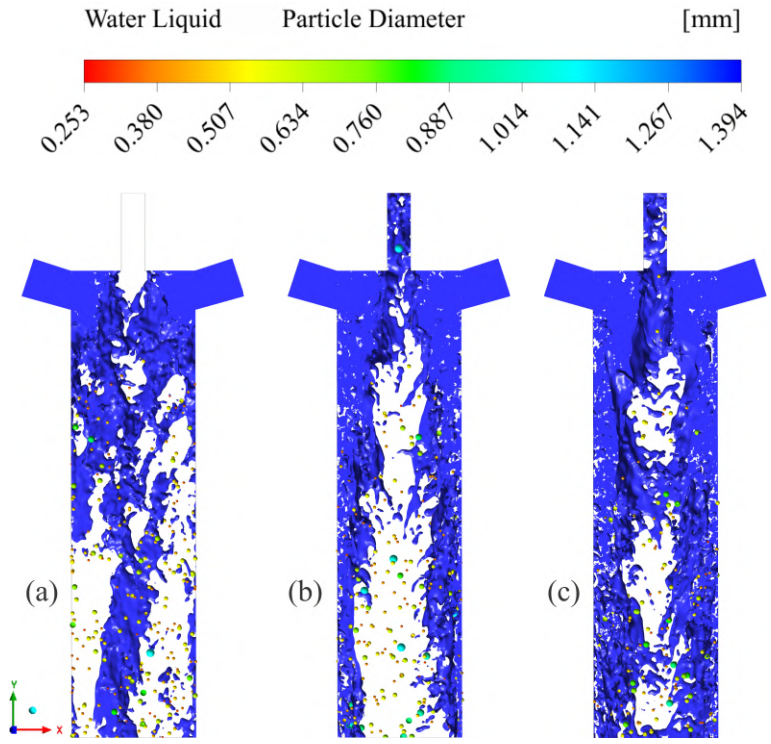

Figure 3. Isosurface of volume fraction of liquid (50%) for Cases a, b and c. Coloured spheres represent Lagrangian particles, with their actual size and coloured by diameter.

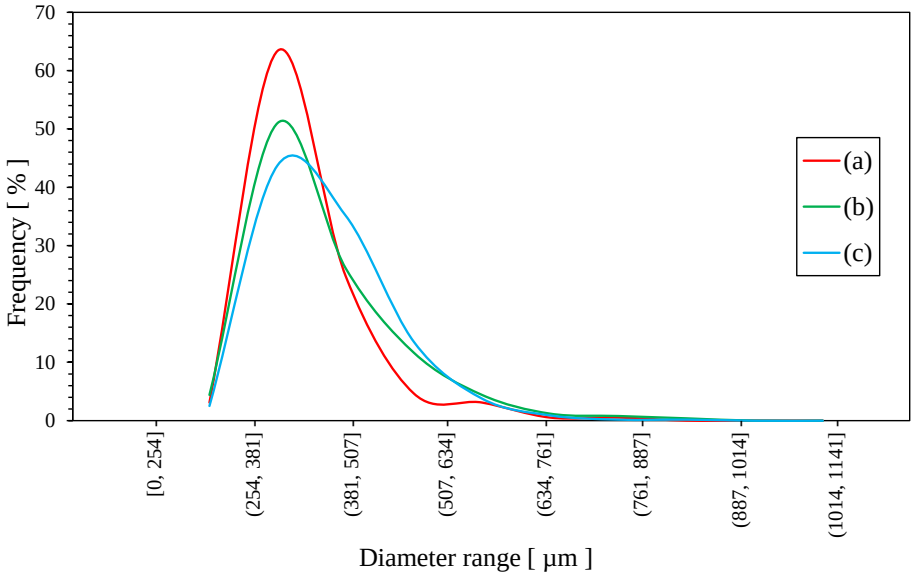

Figure 4. Distribution of Lagrangian droplet diameters at the nozzle outlet for Cases a, b and c.

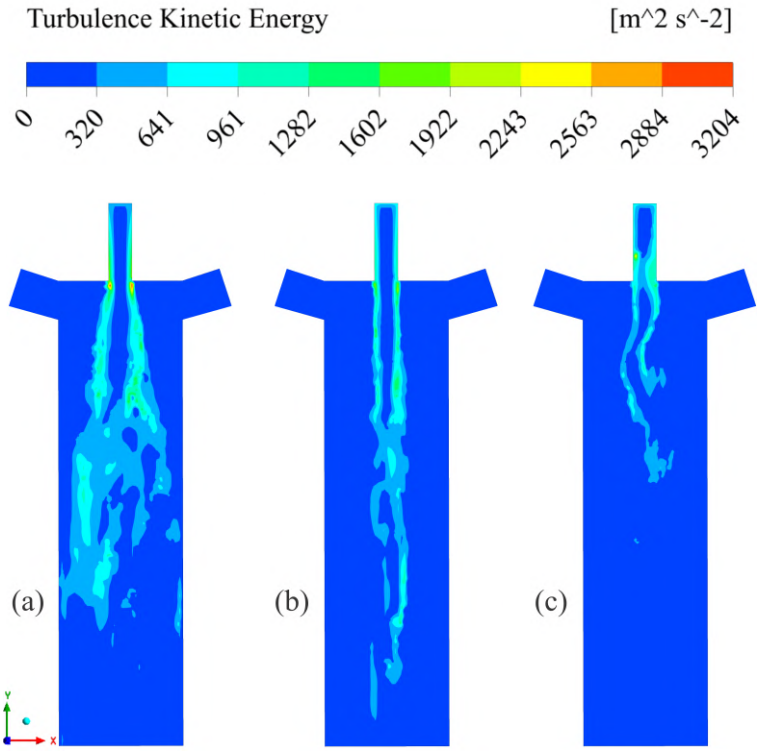

Figure 5. Turbulent kinetic energy distributions for Cases a, b and c.

Regarding the proposed spatial simplification, an expected disadvantage due to the thin mixing chamber would be the increase in the wall effects on the flow. However, the results obtained show that this increase was not large enough to prevent the phenomenon of liquid atomization. Evaluating from a numerical point of view, this geometry enabled the development of a mesh with hexahedral elements with similar volumes – as seen in Fig. 1 – , which directly contributes to the mesh adaptation methodology used. Finally, the set of simplifications due to geometry allowed the results to be obtained in a timely manner.

5. CONCLUSIONS

A numerical study was conducted in order to propose a spatial simplification for simulating a two-fluid nozzle with a pseudo two-dimensional geometry. Due to the complexity of the atomization phenomenon and its different scales of magnitude, this geometric simplification aims to make RANS simulations of spray feasible. For this purpose, considering

air under supersonic conditions and water, simulations were conducted for three different cases. The results showed the great influence of the liquid flow on the characteristics of the obtained sprays and on the distribution of droplet diameters. The contribution of turbulent kinetic energy over the primary breakup was observed, mainly for the case with lower liquid flow. Furthermore, the spatial simplification demonstrated great potential in making the computational effort required in the simulation of sprays viable.

6. ACKNOWLEDGEMENTS

The authors would like to acknowledge the financial support from Petróleo Brasileiro S.A. (PETROBRAS), through the cooperation agreement number 5850.0107354.18.9, and Coordenação de Aperfeiçoamento de Pessoal de Nível Superior – Brasil (CAPES).

7. REFERENCES

Bazdidi-Tehrani, F. and Abedinejad, M.S., 2018. "Influence of incoming air conditions on fuel spray evaporation in an evaporating chamber". *Chemical Engineering Science*, Vol. 189, pp. 233–244. ISSN 00092509. doi: 10.1016/j.ces.2018.05.046.

Catapan, J., 2020. *Avaliação numérica de modelos de quebra secundária para spray do tipo duplo fluido*. Master's thesis, University of Blumenau.

Das, S.K. and Lim, O.T., 2017. "Spray Simulation of n-heptane in a Constant Volume Combustion Chamber over a Wide Range of Ambient Gas Density and Fuel Temperature". *Energy Procedia*, Vol. 105, pp. 1813–1820. ISSN 18766102. doi:10.1016/j.egypro.2017.03.526.

Estivalèzes, J.L., Zuzio, D. and DiPierro, B., 2018. "An improved multiscale Eulerian-Lagrangian method for simulation of atomization process". *Notes on Numerical Fluid Mechanics and Multidisciplinary Design*, Vol. 135, pp. 65–77. doi:10.1007/978-3-319-60387-2_6.

Godoy, V.B., Santos, D.A., Vetter, B.B., Rosa, L.M., Silva, M.K., Utzig, J. and Meier, H.F., 2020. "Experimental investigation of initial disturbances formation, instabilities growth, multiphase turbulence and breakup mechanism inside a mixing chamber of an airassist atomizer". 12th Spring School on Transition and Turbulence.

Jubaer, H., Afshar, S., Xiao, J., Chen, X.D., Selomulya, C. and Woo, M.W., 2019. "On the effect of turbulence models on CFD simulations of a counter-current spray drying process". *Chemical Engineering Research and Design*, Vol. 141, pp. 592–607. ISSN 02638762. doi:10.1016/j.cherd.2018.11.024.

Lefebvre, A. and Mcdonell, V., 2017. *Atomization and Sprays, Second Edition.* CRC press. ISBN 9781498736268. doi:10.1016/0009-2509(90)87140-N.

Mäkelä, M., 2017. "Experimental design and response surface methodology in energy applications: A tutorial review". *Energy Conversion and Management*, Vol. 151, No. September 2017, pp. 630–640. ISSN 01968904. doi: 10.1016/j.enconman.2017.09.021.

Menter, F.R., 1994. "Two-equation eddy-viscosity turbulence models for engineering applications". *AIAA Journal*, Vol. 32, No. 8, pp. 1598–1605. ISSN 0001-1452. doi:10.2514/3.12149.

Neto, P.B., Buss, L., Meierhofer, F., Meier, H.F., Fritsching, U. and Noriler, D., 2018. "Combustion kinetic analysis of flame spray pyrolysis process". *Chemical Engineering and Processing - Process Intensification*, Vol. 129, No. March, pp. 17–27. ISSN 02552701. doi:10.1016/j.cep.2018.04.032.

Reitz, R.D., 1987. "Mechanisms of Atomization Processes in High-Pressure Vaporizing Sprays". *Atomization and Spray Technology*, Vol. 3, pp. 309–337.

Ren, Z., Wang, B., Xiang, G., Zhao, D. and Zheng, L., 2019. "Supersonic spray combustion subject to scramjets: Progress and challenges". *Progress in Aerospace Sciences*, Vol. 105, No. June, pp. 40–59. ISSN 03760421. doi: 10.1016/j.paerosci.2018.12.002.

Salvador, F.J., Gimeno, J., Pastor, J.M. and Martí-Aldaraví, P., 2014. "Effect of turbulence model and inlet boundary condition on the Diesel spray behavior simulated by an Eulerian Spray Atomization (ESA) model". *International Journal of Multiphase Flow*, Vol. 65, pp. 108–116. ISSN 03019322. doi:10.1016/j.ijmultiphaseflow.2014.06.003.

Sanjosé, M., Senoner, J.M., Jaegle, F., Cuenot, B., Moreau, S. and Poinsot, T., 2011. "Fuel injection model for Euler-Euler and Euler-Lagrange large-eddy simulations of an evaporating spray inside an aeronautical combustor". *International Journal of Multiphase Flow*, Vol. 37, No. 5, pp. 514–529. ISSN 03019322. doi: 10.1016/j.ijmultiphaseflow.2011.01.008.

Shinjo, J. and Umemura, A., 2010. "Simulation of liquid jet primary breakup: Dynamics of ligament and droplet formation". *International Journal of Multiphase Flow*, Vol. 36, No. 7, pp. 513–532. ISSN 03019322. doi: 10.1016/j.ijmultiphaseflow.2010.03.008.

Sinnamon, J.F., Lancaster, D.R. and Stiener, J.C., 1980. "An experimental and analytical study of engine fuel spray trajectories". *SAE Technical Papers*. ISSN 26883627. doi:10.4271/800135.

Sun, Y., Alkhedhair, A.M., Guan, Z. and Hooman, K., 2018. "Numerical and experimental study on the spray

characteristics of full-cone pressure swirl atomizers". *Energy*, Vol. 160, pp. 678–692. ISSN 03605442. doi: 10.1016/j.energy.2018.07.060.

Velozo, R.V., 2020. *Simulação numérica da quebra primária de líquido em um dispersor de carga de FCC*. Master's thesis, University of Blumenau.

Verma, N., ManojKumar, K. and Ghosh, A., 2017. "Characteristics of aerosol produced by an internal-mix nozzle and its influence on force, residual stress and surface finish in SQCL grinding". *Journal of Materials Processing Technology*, Vol. 240, pp. 223–232. ISSN 09240136. doi:10.1016/j.jmatprotec.2016.09.014.

Xue, Q. and Kong, S.C., 2009. "Development of adaptive mesh refinement scheme for engine spray simulations". *Computers and Fluids*, Vol. 38, No. 4, pp. 939–949. ISSN 00457930. doi:10.1016/j.compfluid.2008.10.004.

Youngs, D., 1982. "Time-dependent multi-material flow with large fluid distortion". *Num. Method Fluid Dyn.*, Vol. 24, pp. 273–285.

8. RESPONSIBILITY NOTICE

The authors are the only responsible for the printed material included in this paper.